

**Usefulness of real-time tissue elastography for detecting the border of basal cell
carcinomas**

Takamitsu TANAKA, Yayoi TADA, Takamitsu OHNISHI, Shinichi WATANABE

Department of Dermatology, Teikyo University School of Medicine, Tokyo, Japan

Running title: Elastography for BCC border detection

Address correspondence and reprint requests: Takamitsu Tanaka,

Department of Dermatology, Teikyo University School of Medicine, 2-11-1 Kaga,

Itabashi-ku, Tokyo 173-8605, Japan

TEL +81-3-3964-2473, FAX +81-3-5375-5314

E-mail: takamitsu@med.teikyo-u.ac.jp

Abstract

Preoperative evaluation of tumor thickness and silhouette in basal cell carcinoma (BCC) is one of the important assessments to be done. However, evaluation is not always sufficient even utilizing sonography and magnetic resonance imaging. Recently, a new technique called real-time tissue elastography (RTE) was developed that can display the hardness of tissue as a color overlay of a sonography image. Therefore, RTE could be used as a tool for detecting the tumor border according to differences in tissue rigidity. In the present study, the correlation between histopathological and RTE tumor thickness measurements was evaluated for BCCs. Eleven BCCs (6 nodular type, 3 superficial type, and 2 adenoid or cystic type) from individual patients were evaluated. Tumor silhouette and thickness were detected using conventional B-mode sonography and RTE. All lesions were surgically excised and tumor thickness was also examined histologically. In the 6 nodular type BCCs, the tumor silhouette determined by RTE showed a close correlation with the results of histopathology. Particularly, for 4 out of the 6 cases, the correlation was excellent. In addition, the mean difference in tumor thickness measurements between histology and RTE (-0.368 mm) was lower than that between histology and B-mode sonography (-0.835 mm). As for the superficial type BCCs, tumor thickness was too thin to evaluate. Tumor thickness measured by B-mode sonography and RTE was identical for 2 cases of adenoid or cystic type BCC. In conclusion, RTE is useful in the preoperative assessment of tumor thickness, especially with the nodular type of BCC, and allows us to determine adequate surgical margins.

Key words

Basal cell carcinoma, elastography, sonography, surgical margin, tumor thickness

Introduction

Accurate evaluation of preoperative tumor extent is important for determining appropriate surgical treatment. The recurrence rate of BCC was reported to be 10%¹, and most recurrences are thought to occur due to tumor resection with an insufficient surgical margin. Since determining the surgical margin of residual BCC is difficult, extensive resection would be needed in the subsequent operations of such recurrent cases. In order to evaluate tumor extent accurately, high-frequency sonography^{2,3}, dermoscopy⁴, and magnetic resonance imaging⁵ are commonly used. Among these techniques, ultrasonographic examination is convenient, noninvasive, inexpensive, and can detect the tumor silhouette from all directions of imaging. Although 13- or 20-MHz sonography have been used to evaluate BCC extent, high-frequency sonography has recently been used more frequently because of having a higher resolution. In addition, the sonographic technique of real-time tissue elastography, which can display tissue rigidity as a color overlay of the tissue image, has been developed. This technique is based on the principle that softer tissue deforms more easily than harder tissue when gentle compression is applied through manual freehand operation⁶. The purpose of this study is to evaluate the benefit of real-time tissue elastography for assessing the tumor silhouette and thickness of BCC noninvasively before operation.

Methods

Patients

A total of 11 patients with BCC (6 nodular type, 3 superficial type, and 2 adenoid or cystic type) who were referred to the Department of Dermatology, Teikyo University Hospital from July to December 2014 were included in this study. The patients consisted

of 7 males and 4 females aged 38–87 years (the mean age was 63.9 years). The anatomical locations of BCC were 7 on the head and/or neck, 2 on the trunk, 1 on the lower limbs, and 1 on the genitalia.

Ultrasonographic equipment

A sonographic scanner (Noblus; Hitachi-Aloka Medical, Ltd., Tokyo, Japan) with two probes (3–7 MHz and 5–13 MHz) was used to obtain B-mode images. Standard sonographic gel was applied on the tumor surface, and a water pad was also used to cover the probe surface. A sonographic examination was performed to visualize the echostructures of the entire lesion. The recorded images were adjusted by gain curve to obtain the best contrast. When the probe was attached to the target region, the B-mode image by the sonographic scanner appeared on the right side of the screen. At the same time, elastographic image appeared on the left side of the screen. That is, elastographic images were also examined under the same conditions of time, probes, and locations with B-mode. The images showed the differences in tissue rigidity by color, namely red as soft, yellow to green as moderate, and blue as hard. Tumor thickness was measured by both conventional B-mode sonography and elastography.

Histopathologic evaluation

Excised BCC specimens were fixed in 10% (w/v) neutral buffered formalin, embedded in paraffin, and then stained using hematoxylin-eosin. These slides were scanned by virtual slide-scanner (NanoZoomer-XR; Hamamatsu Photonics, Hamamatsu City, Japan) and the border of the tumor was traced by a line to define the silhouette of the BCC. The most thickened part of the tumor was measured within the scanned images.

Results

Nodular type BCC

Within 6 nodular type BCC samples (Cases 1–6; Table 1), conventional B-mode sonography showed well-demarcated hypoechoic structures (Figs. 1–3). The results of evaluating tumor thickness using ultrasonographic equipment compared with actual histologic thickness are summarized in Table 1. With Cases 1 and 3, the extent of BCC was detected more accurately with elastography compared to conventional B-mode sonography. With these 6 nodular type cases, the mean value of differences in tumor thickness between histology and B-mode sonography was -0.835 mm, while that between histology and elastography was -0.368 mm. Thus, tumor thickness evaluation using elastography was more accurate than that using B-mode sonography for nodular type BCCs. For example, the BCC silhouette indicated by arrows in Figs. 1b (left) and 1c was shown as a blue hard area by elastography, but could not be detected by B-mode sonography (Fig. 1b, right). Nodular BCC accompanied by ulcer (Case 6; Table 1), was displayed as a mixture of green, yellow, and red coloration by elastography (Fig. 3b, left) indicating soft~moderate tissue rigidity.

Superficial type BCC

With 3 cases of superficial type BCC, evaluation by sonography showed thin hypoechoic structures. The extent of each BCC was shown as a diffuse blue area via elastography (Fig. 4b, left) and a black area by B-mode sonography (Fig. 4b, right), which is traced by a black line in the histopathology image (Fig. 4c). This area contains not only the BCC but also inflammatory cell infiltration into the upper dermis (Fig. 4d). Therefore, the actual tumor thickness was not accurately detected by either B-mode sonography or

elastography. The histological tumor thickness was 0.423 mm, and the thickness of the area traced by a dotted line based on evaluation by elastography and B-mode sonography was 0.2 mm (Figs. 4b and c).

Adenoid or cystic type BCC

With 3 cases of adenoid or cystic type BCC, evaluation by B-mode sonography showed hypoechoic structures intermingled with some brighter areas, indicating calcification or keratinizing cysts, and small hypoechoic areas (Fig. 5). This hypoechoic structure was demonstrated as a dark blue rigid area by elastography. Within this area, cysts were shown as red spots and adenoid structures adjacent to cysts were shown as yellow to green areas. Thus, elastography was more informative regarding the detailed structure of adenoid or cystic type BCC than B-mode sonography was. However, tumor thickness measurements by both B-mode sonography and elastography were the same as the actual histological thickness, suggesting no advantage of elastography over B-mode sonography for measuring the extent of adenoid or cystic type BCC.

Discussion

Real-time tissue elastography is a novel ultrasonography technique that can differentiate tissues according to their stiffness. Since healthy tissues are usually softer than tumorous tissues⁷, elastography has been suggested to be useful for tumor diagnosis. For example, breast cancer is harder than surrounding normal breast tissue; therefore, elastography has been shown to be useful for diagnosing breast cancer and evaluating its extent⁸. Likewise, sonographic elastography has been already used to diagnose and examine cancers of several other organs, namely thyroid⁹, prostate¹⁰, cervix¹¹, and liver¹². In addition, it has been reported to be

useful for detecting lymph node metastases of malignant melanoma¹³ and squamous cell carcinoma¹⁴, and for diagnosing the cause of enlarged cervical lymph nodes¹⁵. In the present study, we evaluated the tumor silhouette and thickness of 11 cases of BCC utilizing this new approach.

Here, we demonstrated that the tumor thickness of nodular BCCs measured by elastography correlated better with the histological thickness than the tumor thickness measured by conventional B-mode sonography did. The mean value of differences in thickness measurements of 6 BCCs between histology and elastography evaluations was -0.368 mm, which was smaller than that between histology and B-mode sonography evaluation (-0.835 mm). In addition, we showed that elastography was better for detecting the tumor silhouette of nodular BCC in detail. However, in 2 cases of nodular BCCs, elastographic images were not superior to B-mode sonography images. One case was BCC on the nose tip, and the other case was BCC with ulcer. We speculate that when the probe could not be attached uniformly due to the anatomical location of BCC, such as the case with a round surface on the nose, the accuracy of elastography evaluation could be disturbed. In the case of BCC with ulcer, we speculate that because of the inflammation and tissue destruction, tumor rigidity changes resulted in a decreased accuracy of elastography evaluation.

Within the superficial BCCs, the tumor thickness was too thin to be differentiated as a region of different rigidity from the surrounding dermis with dense inflammatory cell infiltration. Indeed, elastography images revealed diffuse blue areas, which included the surrounding upper dermis with cell infiltration. The tumor silhouette detected by conventional B-mode sonography was the same, and the B-mode images also demonstrated a 0.2 mm layer of inflammatory cell infiltration as a black area. Thus,

sonography is not useful for evaluating the thickness of superficial BCC with cell infiltration.

In the adenoid or cystic BCCs, the tumor silhouette and thickness detected by B-mode sonography and elastography were similar. However, some small green, yellow, or red spots were seen in elastographic images that corresponded to necrosis of tumor nests or liquid accumulation in cysts. Since these features would make the border of the tumor obscure, we should be careful when evaluating the extent of adenoid or cystic BCCs by elastography.

There are some limitations in this study. First of all, since there was no case showing tumor invasion into the subcutaneous tissue in the present study, we still have not answered the question of whether elastography would be useful for detecting tumor invasion into the subcutaneous tissue. Except for the case of BCC on the nose where adipose tissue is scarce, the adipose tissue was shown as red or yellow areas. Since the nests of BCC could be detected as blue or green areas, elastography might be useful for evaluating BCC infiltration into the adipose tissue or muscle. Secondly, morphemic type BCC is another type of BCC that was also not included in the present study. We still do not know whether real-time elastography is useful enough to detect the firmness of morphemic type BCC. Thirdly, if we have used the higher-frequency sonography, clearer image might have been obtained even by B-mode. We would like to examine these speculations in future studies.

Here, we studied the benefit of using elastography for BCC evaluation. This technique could be beneficial for evaluating other skin tumors, especially those with a firm consistency. Shear-wave elastography¹⁶ is another recently developed elastography technique that can quantify rigidity through mechanical vibration. We expect that this newly-developed elastography technique will enable us to more accurately evaluate and

diagnose skin tumors, including BCC.

Acknowledgement

None

Conflict of Interest Statemt

None

References

1. Mosterd K, Krekels GA, Nieman FH, Ostertag JU, Essers BA, Dirksen CD, Steijlen PM, Vermeulen A, Neumann H, Kelleners-Smeets NW. Surgical excision versus Mohs micrographic surgery for primary and recurrent basal-cell carcinoma of the face: a prospective randomized trial with 5-year' follow-up. *Lancet Oncol* 2008; 9: 1149-56.
2. Lassau N, Spatz A, Avril MF, Tardivon A, Margulis A, Mamelle G, Vanel D, Leclere J. Value of high-frequency US for preoperative assessment of skin tumors. *Radiographics* 1997; 17: 1559-1565.
3. Gupta AK, Turnbull DH, Foster FS, Harasiewicz KA, Shum DT, Prussick R, Watteel GN, Hurst LN, Sauder DN. High frequency 40-MHz ultrasound. A possible noninvasive method for the assessment of the boundary of basal cell carcinomas. *Dermatol Surg* 1996; 22: 131-136.
4. Marghoob AA, Braun R. Proposal for arevised 2-step algorithm for the classification of lesions of the skin using dermoscopy. *Arch Dermatol* 2010; 146: 426-428.
5. Gufler H, Franke FE, Rau WS. High-resolution MRI of basal cell carcinomas of the face using a microscopy coil. *Am J Roentgenol* 2007; 188: w480-w484.
6. Ophir J, Céspedes I, Ponnekanti H, Yazdi Y, Li X. Elastography. A quantitative method for imaging the elasticity of biological tissues. *Ultrason Imaging* 1991; 13: 111-134.
7. Céspedes I, Ophir J. Reduction of image noise in elastography. *Ultrason Imageing* 1993; 15: 89-102.
8. Thomas A, Fischer T, Frey H, Ohlinger R, Grunwald S, Blohmer JU, Winzer KJ, Weber S, Kristiansen G, Ebert B, Kümmel S. Real-time elastography an advanced

method of ultrasound: first results in 108 patients with breast lesions. *Ultrasound Obstet Gynecol* 2006; 28: 335-340.

9. Asteria C, Giovanardi A, Pizzocaro A, Cozzaglio L, Morabito A, Somalvico F, Zoppo A. US-elastography in the differential diagnosis of benign and malignant thyroid nodules. *Thyroid* 2008; 18: 523-531.
10. Taylor LS, Rubens DJ, Porter BC, Wu Z, Baggs RB, di Sant'Agnese PA, Nadasdy G, Pasternack D, Messing EM, Nigwekar P, Parker KJ. Prostate cancer: three-dimensional sonoelastography for in vitro detection. *Radiology* 2005; 237: 981-985.
11. Thomas A, Kümmel S, Gemeinhardt O, Fischer T. Real-time sonoelastography of the cervix: tissue elasticity of the normal and abnormal cervix. *Acad Radiol* 2007; 14: 193-200.
12. Friedrich-Rust M, Ong MF, Herrmann E, Dries V, Samaras P, Zeuzem S, Sarrazin C. Real-time elastography for noninvasive assessment of liver fibrosis in chronic viral hepatitis. *Am J Roentgenol* 2007; 188: 758-764.
13. Hinz T, Hoeller T, Wenzel J, Bieber T, Schmid-Wendtner MH. Real-time elastography as promising diagnostic tool for diagnosis of lymph node metastases in patients with malignant melanoma: A prospective single-center experience. *Dermatology* 2013; 226: 81-90.
14. Aoyagi S, Izumi K, Hata H, Kawasaki H, Shimizu H. Usefulness of real-time tissue elastography for detecting lymph-node metastases in squamous cell carcinoma. *Clin Exp Dermatol* 2009; 34: e744-e747.
15. Alam F, Naito K, Horiguchi J, Fukuda H, Tachikake T, Ito K. Accuracy of sonographic elastography in the differential diagnosis of enlarged cervical lymph nodes: comparison with conventional B-mode sonography. *Am J Roentgenol* 2008; 191: 604-

16. Bercoff J, Tanter M, Fink M. Supersonic shear imaging: A new technique for soft tissue elasticity mapping. *IEEE Trans Ultrason Ferroelectr Freq Control* 2004; 51: 396–409.

Table 1

Histopathological type and tumor thickness of BCCs examined in this study.

Figure legends

Figure 1

- (a) Clinical appearance of Case 1. A light red–brown and partially black-pigmented, hard, well-demarcated skin tumor composed of multiple waxy small nodules on the back. The area marked by a blue rectangle was evaluated by sonography and the results were compared with those of histopathological examination.
- (b) Skin ultrasound examination by B-mode sonography (right) showed a well-demarcated hypoechoic structure, which was detected as a dark blue area by elastography (left). The adjacent blue areas (arrows) were detected only by elastography. The dermis appeared as a green area, and the subcutaneous fat appeared as yellow and red areas.
- (c) Histopathology of the nodular BCC with hematoxylin and eosin staining. The lesions marked by arrows in the elastography images correlated with the downward extensions of the BCC observed by histopathological examination.

Figure 2

- (a) Clinical appearance of Case 3. A brown and partially black-pigmented, hard skin nodule composed of two small nodules with an ulcer on the cheek. The area marked by a blue rectangle was evaluated by sonography and the results were compared with those of histopathological examination.
- (b) Skin ultrasound examination by B-mode sonography (right) showed a well-

demarcated hypoechoic structure, which was detected as a dark blue area by elastography (left). The adjacent blue areas (arrows) were detected only by elastography. The dermis appeared as a green area, and subcutaneous fat appeared as yellow and red areas.

- (c) Histopathology of the nodular BCC with hematoxylin and eosin staining. The lesions marked by arrows in the elastography images correlated with the downward extensions of the BCC observed by histopathological examination.

Figure 3

- (a) Clinical appearance of Case 6. A black-pigmented skin nodule with a rolled edge and central ulceration on the forehead. The area marked by a blue rectangle was evaluated by sonography and the results were compared with those of histopathological examination.
- (b) Skin ultrasound examination by B-mode sonography (right) showed a well-demarcated hypoechoic structure, which was detected as an area of mixed green, yellow, and red colors via elastography (left). The dermis appeared as a green area, and the subcutaneous fat appeared as yellow and red areas.
- (c) Histopathology of the nodular BCC with hematoxylin and eosin staining. The center of tumor is necrotized and ulcerated with inflammatory cell infiltration.

Figure 4

- (a) Clinical appearance of Case 7. An erythematous plaque with black-pigmented dots on the abdomen. The area marked by a blue rectangle was evaluated by sonography and the results were compared with those of histopathological

examination.

- (b) Skin ultrasound examination by B-mode sonography (right) showed a thin hypoechoic structure, which was detected as diffuse blue areas by elastography (left), which include the surrounding dermis with cell infiltration. The dermis appeared as a blue area, and the subcutaneous fat appeared as yellow and red areas. The tumor thickness is indicated by a red two-headed arrow.
- (c) Histopathology of the superficial BCC with hematoxylin and eosin staining and at high: $\times 400$ magnification magnification.
- (d) Histopathology of the superficial BCC with hematoxylin and eosin staining and at low: $\times 100$ magnification magnification. The tumor thickness is indicated by a red two-headed arrow. The thickness of inflammatory cell infiltration is 0.2 mm, as indicated by a two-headed green arrow.

Figure 5

- (a) Clinical appearance of Case 11. A brownish nodule with black-pigmented dots and some scales on the cheek.
- (b) Skin ultrasound examination by B-mode sonography (right) showed hypoechoic structures including some high brightness and small hypoechoic areas, which were detected as blue areas with some small green, yellow, or red spots by elastography (left). The dermis appeared as a green area, and the subcutaneous fat appeared as green, yellow, and red areas.
- (c) Histopathology of the adenoid or cystic BCC with hematoxylin and eosin staining.

Table 1 Histopathological type and tumor thickness of BCCs examined in this study

Case	age	sex	location	histopathological type	Thickness by B-mode (mm)	Thickness by elastography (mm)	Histopathological thickness (mm)
1	62	M	back	nodular	2.0 (−2.0)	4.0 (0.0)	4.00
2	80	M	pelvis	nodular	7.0 (0.0)	7.0 (0.0)	7.00
3	75	M	cheek	nodular	1.2 (−1.41)	2.0 (−0.61)	2.61
4	38	F	head	nodular	5.0 (−0.3)	5.0 (−0.3)	5.30
5	87	F	nose	nodular	3.0 (−1.0)	3.0 (−1.0)	4.00
6	87	F	forehead	nodular	4.0 (−0.3)	4.0 (−0.3)	4.30
7	57	M	abdomen	superficial	0.6 (−0.17)	-	0.43
8	81	M	pubis	superficial	1.02 (0.0)	-	1.02
9	68	M	thigh	superficial	1.2 (+0.21)	-	1.41
10	67	F	cheek	adenoid or cystic	2.3 (−0.02)	2.3 (−0.02)	2.32
11	72	M	cheek	adenoid or cystic	5.9 (0.0)	5.9 (0.0)	5.90

- : not detected
() : Mean value of difference in thickness compared with histopathological evaluation

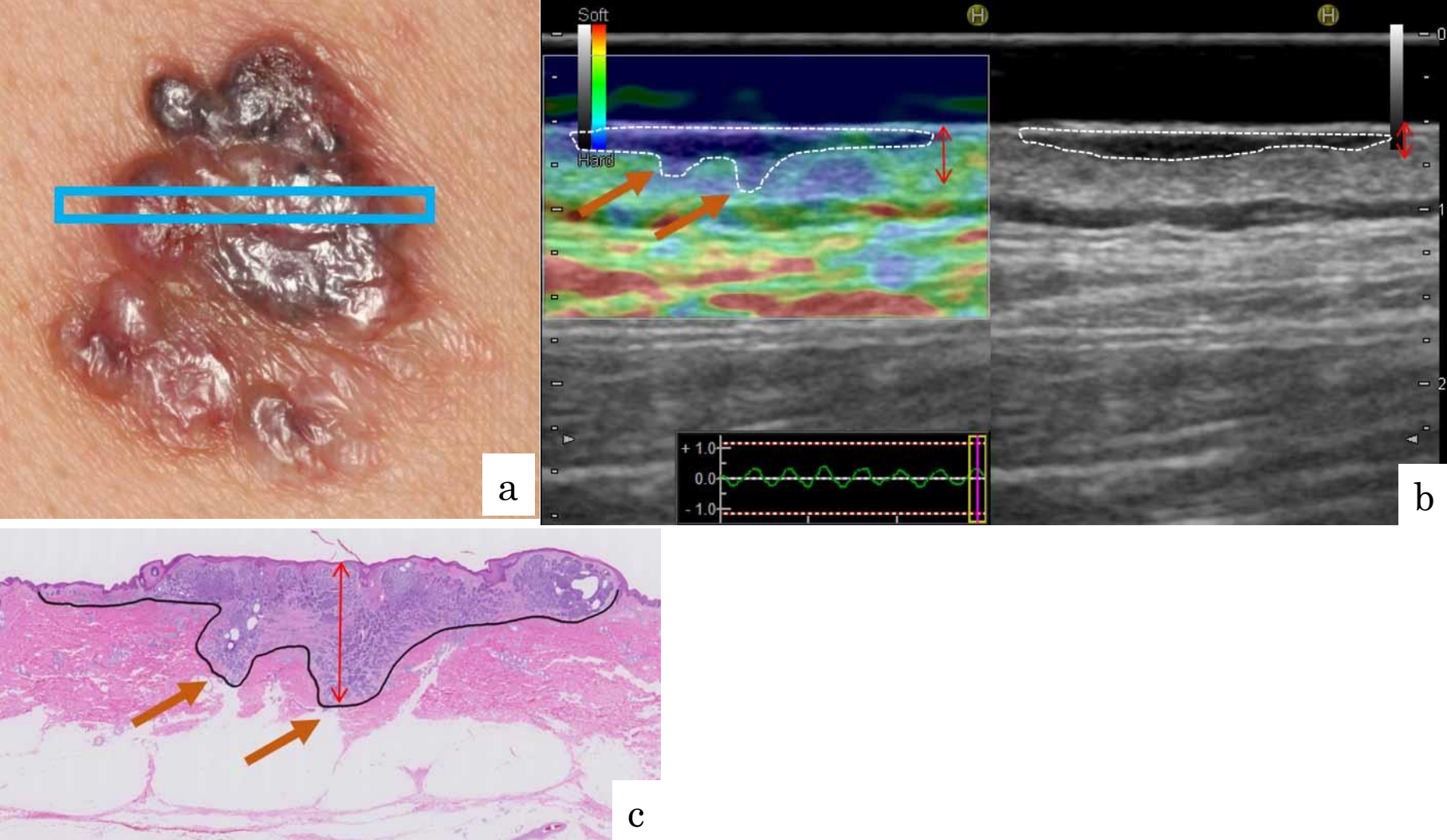


Figure 1
Tanaka T et al.

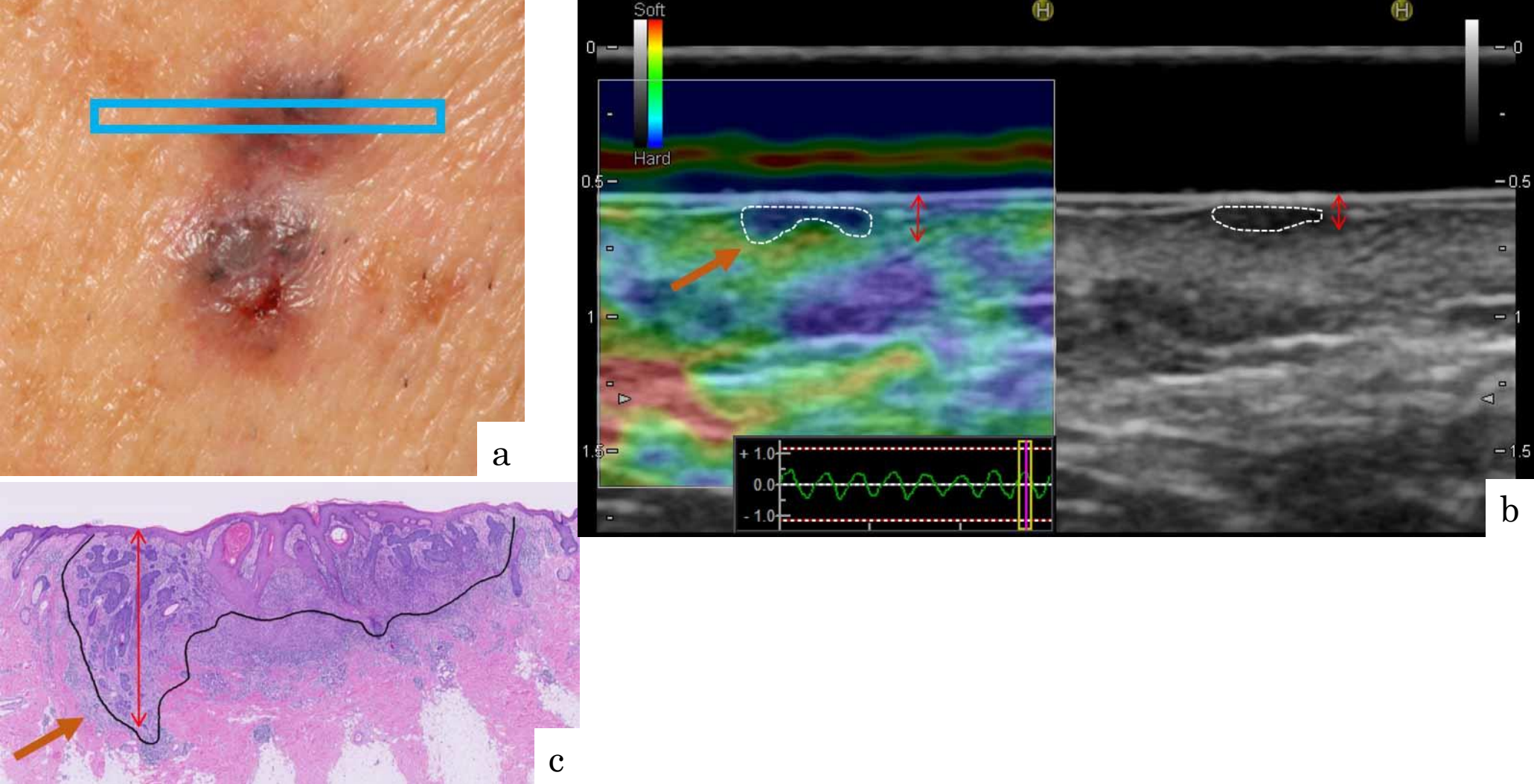


Figure 2
Tanaka T et al.

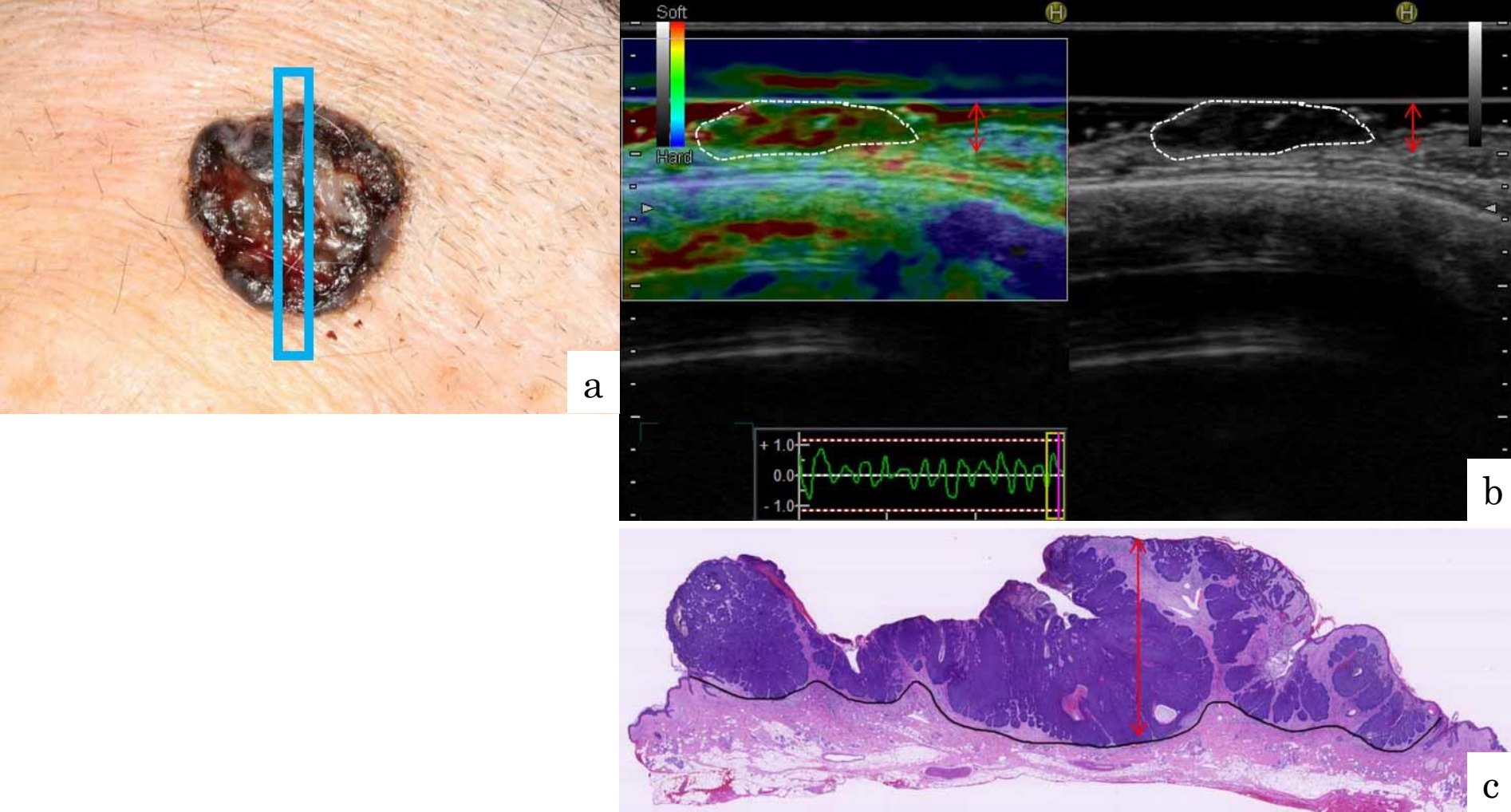


Figure 3
Tanaka T et al.

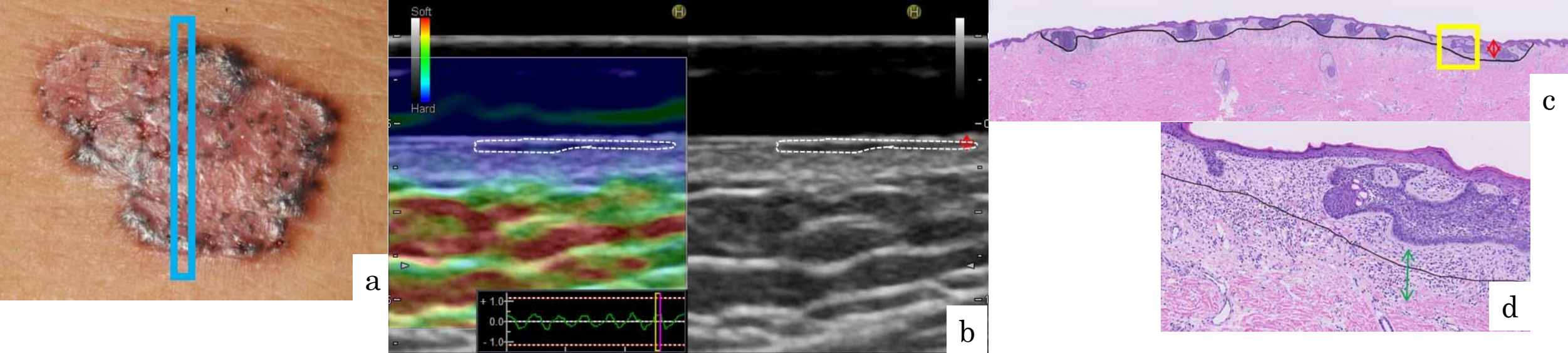


Figure 4
Tanaka T et al.

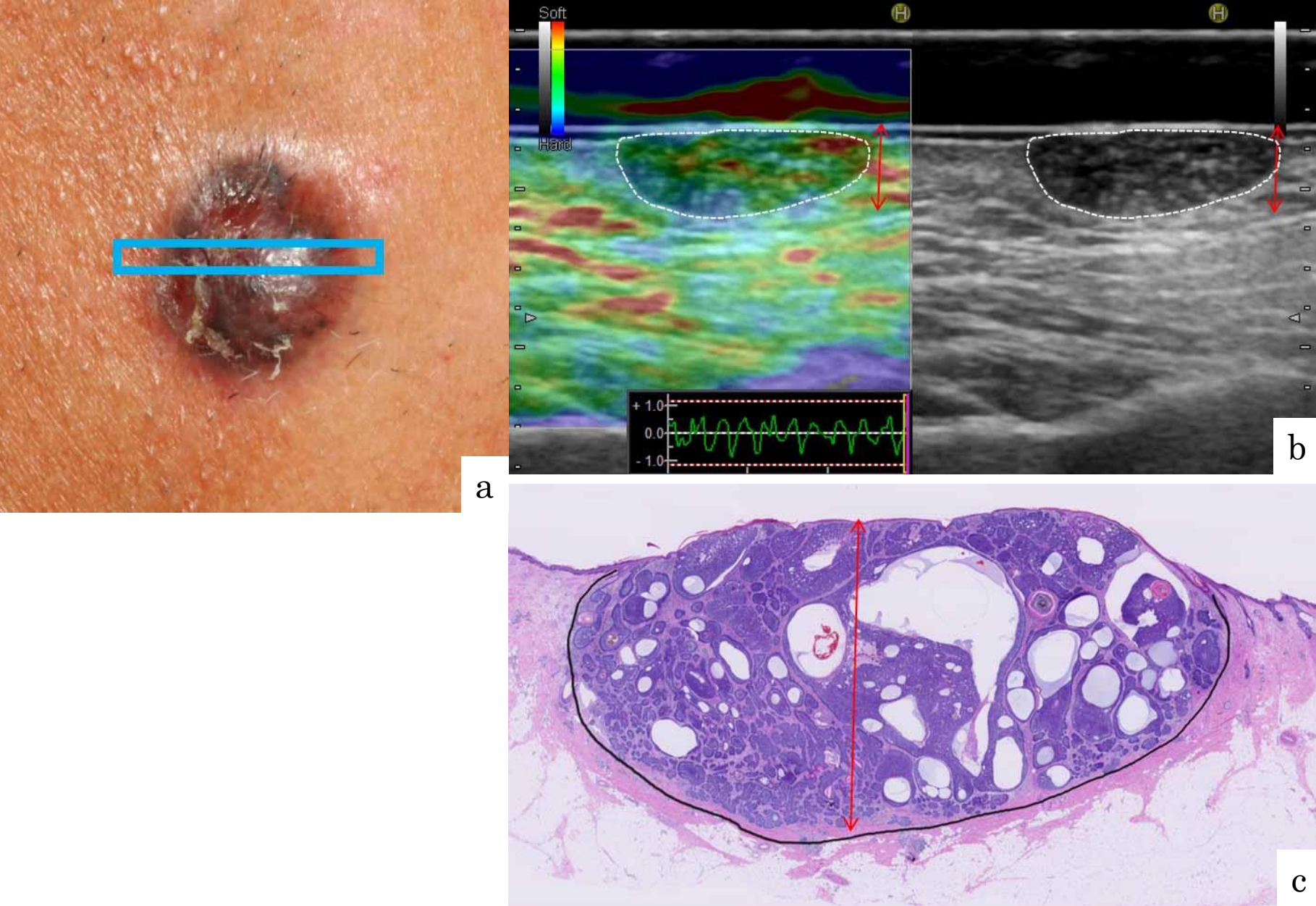


Figure 5
Tanaka T et al.